Quantifying effects of conservation practices on non-point source pollution in the Miyun Reservoir Watershed, China

Jiali Qiu · Zhenyao Shen · Lei Chen · Xiaoshu Hou

Abstract Non-point source (NPS) pollution, including fertilizer and manure application, sediment erosion, and haphazard discharge of wastewater, has led to a wide range of water pollution problems in the Miyun Reservoir, the most important drinking water source in Beijing. In this study, the Soil and Water Assessment Tool (SWAT) model was used to evaluate NPS pollution loads and the effectiveness of best management practices (BMPs) in the two subwatersheds within the Miyun Reservoir Watershed (MRW). Spatial distributions of soil types and land uses, and changes in precipitation and fertilizer application, were analysed to elucidate the distribution of pollution in this watershed from 1990 to 2010. The results demonstrated that the nutrient losses were significantly affected by soil properties and higher in both agricultural land and barren land. The temporal distribution of pollutant loads was consistent with that of precipitation. Soil erosion and nutrient losses would increase risks of water eutrophication and ecosystem degradation in the Miyun Reservoir. The well-calibrated SWAT model was used to assess the effects of several Best Management Practices (BMPs), including filter strips, grassed waterways, constructed wetlands, detention basins, converting farmland to forest, soil nutrient management, conservation tillage, contour farming, and strip cropping. The removal rates of those BMPs ranged from 1.03 to 38.40% and from 1.36 to 39.34% for total nitrogen (TN) and total phosphorus (TP) loads, respectively. The efficiency of BMPs was dependent on design parameters and local factors and varied in different sub-basins. This study revealed that no single BMP could achieve the water quality improvement targets and highlighted the importance of optimal configuration of BMP combinations at sub-basin scale. The findings presented here provide valuable information for developing the sustainable watershed management strategies.

Keywords Non-point source pollution · SWAT · Spatial distribution · Temporal distribution · Miyun Reservoir Watershed · Best management practice

Introduction

Agricultural non-point source (NPS) pollution has been a significant threat to water quality and ecosystem of the Miyun Reservoir in recent decades. Runoff leaching from fertilizers and livestock litter contribute to high nutrient levels in some rivers in the agricultural areas, which lead to a wide range of risks associated with eutrophication and toxicity of water bodies and inadequate water supply quality for Beijing (Li et al. 2016; Meissner et al. 2016). Implementation of sustainable land-management practices or conservation practices is becoming an important concern to control NPS pollution in the Miyun Reservoir Watershed (MRW). However, before the selection and placement of suitable management practices in this watershed, it requires a

J. Qiu · Z. Shen (✉) · L. Chen · X. Hou
State Key Laboratory of Water Environment Simulation, School of Environment, Beijing Normal University, People's Republic of, Beijing 100875, China
e-mail: zyshen@bnu.edu.cn

detailed investigation of the extent, distributions and causes of the pollution, and the effectiveness of alternative practices.

The complexity and uncertainties related to the sources, generation, and transport of NPS pollution lead to numerous difficulties in quantifying pollution characteristics and efficiency of best management practices (BMPs) (Arnold et al. 2012b; Qiu et al. 2018b). A mass of research has relied on watershed models or water quality models, such as the Soil and Water Assessment Tool (SWAT) model (Arnold et al. 1998), the Storm Water Management Model (SWMM) (Huber et al. 1975), and the annualized Agricultural Non-Point Source Pollution Model (AnnAGNPS) (Cronshey and Theurer 1998), to thoroughly study NPS pollution characteristics and the impacts of management practices on sediment and nutrient loss at watershed scale. The SWAT model has been applied in numerous studies because of its open code source, its high accuracy (Arnold et al. 1998), and its strengths in performing calibration and validation, and analyzing parameter sensitivity and uncertainty (Abbaspour et al. 2015). Reliable representation of BMPs in models is critical for credible simulation of BMP efficiency. Multiple efforts have proven SWAT's capability of simulating BMP effects on hydrology and water quality in the watershed processes (Abbaspour et al. 2015; Liu et al. 2018; Volk et al. 2016; Yen et al. 2016). Xie et al. (2015) stated that the SWAT model could simulate more types of BMPs than other models such as HSPF, AGNPS, and AnnAGNPS, including grazing management, grade stabilization structure, and stream channel stabilization. The SWAT model simulates the efficiency of conservation practices by changing the input data or parameters and by operating specific modules. The SWAT-CUP program enables sensitivity analysis, calibration, and uncertainty analysis of SWAT model by linking five optimization procedures, including SUFI2, ParaSol, PSO, GLUE, and MCMC (Abbaspour et al. 2007). In this study, the SUFI2 program was used for parameter sensitivity analysis and model calibration, considering its high effectiveness in calibration and uncertainty analysis (Akhavan et al. 2010; Faramarzi et al. 2009).

BMPs for agricultural NPS pollution have primarily focused on the control of soil erosion and fertilizer amount in China. Traditional practices, including conservation tillage, crop rotation, contour farming, and nutrient management, have been widely implemented in recent years (Jia et al. 2019; Liu and Huang 2013;

Smith and Siciliano 2015; Sun et al. 2018). They protect the land surface by limiting soil-disturbing activities, reduce erosion by improving soil structure, and control the source of pollutants by managing the amount of fertilizes (Logan 1993; Prosdocimi et al. 2016; Zhu et al. 2015). Because of the increasing attention on NPS pollution, structural practices including the terraces, constructed wetlands, grassed waterways, and filter strips are widely implemented, especially for stormwater management (Fonseca et al. 2018; Small et al. 2018). These practices are constructed to reduce runoff through increased infiltration (Logan 1993), to absorb nutrients or other pollutants by specific perennial plants and to reduce soil erosion through decreasing the slope. Multiple watershed models are extensively used to evaluate the performance of BMPs. The SWAT model has been demonstrated to be an effective tool to evaluate the effects of alternative management practices on water resources across watershed and regional scales.

The Miyun Reservoir is stressed by an increasing drinking water supply for a large population of 21.75 million in Beijing. Unpredictable changes related climate, land cover, agricultural activities, and pollution sources pose a challenge for freshwater supplies, in view of the high concentration of nitrogen that is near the eutrophication standards (Li et al. 2016; Qiu et al. 2019; Xia et al. 2015; Zheng et al. 2016). The development of integrated water management strategies is necessary to avoid the risk of inadequate water quantity and quality, which thus can ensure freshwater provisioning and improve ecosystem services (Abbaspour et al. 2015; Ferreira et al. 2019; Halbe et al. 2018). The goal of this study was to use SWAT to simulate the hydrological and water quality processes and to assess the efficiencies of several conservation practices at the sub-basin level and monthly time intervals in a large-scale watershed. The objective of this study can be achieved by the following tasks: (1) analyze the parameter sensitivities in the different subwatersheds; (2) identify the spatial-temporal distributions and priority control areas of different pollutants; (3) analyze the causal factors for the spatial-temporal distributions of nutrient loads; (4) assess the effects of conservation practices or BMPs on agricultural NPS pollution. In particular, variations in the efficiency of different practices were analyzed based on surface conditions, pollution characteristics, climate features, and BMP design parameters. The results of this study provide consistent information on the temporal and spatial distributions of the quantity and quality of water

resources, highlight the sources of contamination, describe the impact of climate and land use change on water resources, identify the applicability of conservation practices, and eventually provide valuable information for the development of integrated watershed management strategies.

Materials and methods

Watershed description

The Miyun Reservoir is the most important surface drinking water source in China's capital, Beijing. The MRW (40° 19′~41° 36′ N, 115° 27′~117° 35′ E) is a drained watershed of the Miyun Reservoir, covering two tributaries: the Chao River and the Bai River. This watershed encompasses forests, agricultural areas, pastureland, streams, and industrial and residential sites, with a total area of approximately 14,923.95 km^2. The Chao River subwatershed covers an area of 5892.97 km^2, and the Bai River subwatershed covers an area of 9030.98 km^2 (see Fig. 1). The average annual temperature observed in the period of 1960–2014 is approximately 8.5–12 °C, with extreme low temperatures below − 30 °C and extremely high temperatures 39 °C. The average annual precipitation is 660 mm, and about 80% of the precipitation occurs from June to September. Agriculture and economic forest planting are the main economic activities in the region. The massive application of fertilizers and manures has caused a great release of nitrogen (N) and phosphorus (P) into the streams, aggravating the risk of eutrophication in the Miyun Reservoir. Therefore, it is important to implement appropriate conservation practices to control nutrient losses for ensuring drinking water security in this area.

Model description

The SWAT model was developed to evaluate water quality, NPS pollution, and the impacts of management practices on water resources at watershed scale. It is a conceptual, semi-distributed, continuous time model at daily, monthly, or annual time intervals developed by USDA Agricultural Research Service (USDA-ARS) and Texas A&M AgriLife Research (Arnold et al. 1998; Srinivasan et al. 1998). The input data for the SWAT simulation is shown in Table 1. Digital Elevation Model (DEM) data with a 90-m grid were used to divide the watershed into multiple sub-basins and to extract the information of channel length and average slope in each sub-basin. Sub-basins were then further subdivided into hydrologic response units (HRUs), which are the smallest unique computational units that combine topographical, land covers, crop types, management operations, and soil characteristics with homogeneous hydrologic response for the simulation of flow and pollutant loads (Ahmadzadeh et al. 2016; Molina-Navarro et al. 2016). In this study, land use data (1:100,000) were provided by the Institute of Geographical and Natural Resources Research, China, and were categorized in the map that consisted of forest-mixed land (49.24%), agricultural land (21.54%), grassland (27.33%), open water (1.18%), industrial and residential land (0.55%), and barren land (0.16%). FAO soil (http://www.fao.org/soils-portal/soil-survey/soil-maps-and-databases/en/) was categorized into 14 types, which is shown in Fig. S2 in the Supplementary Material. Local weather data were obtained from weather stations available in this watershed, including daily rainfall, relative humidity, maximum and minimum temperatures, solar radiation, and wind speed. Monthly flow and water quality data (sediment, N and P loads) were provided by local environmental monitoring stations. The calibration and validation of the flows and nutrient loads were performed for 1990–1998 and 1999–2010, respectively, whereas the periods for sediment calibration and validation were 2006–2008 and 2009–2010, respectively, due to limitations of the data. Other input data for the SWAT model, including livestock amounts, crop types, tillage patterns, the types, amount and timing of fertilizer, manure and pesticide application, social economics, and population were collected by field investigations and from statistical yearbooks that were published by the National Bureau of Statistics. Based on the results of on-site questionnaire survey, corn is the main crop usually grown in this area, and 325 kg/ha of fertilizer is applied in cropping land per year, mainly in May and October when approximately 200 kg/ha of fertilizer or manure are applied in the walnut and chestnut forests. Tillage type for corn is ploughing before sowing without mulching film. We assume that irrigation is only available in combination with fertilization, with unlimited volume up to the maximum annual value of 500 mm. Corn, chestnuts, and walnuts are harvested in September. Taking into account the independence and the differences in surface characteristics and water quality between the two subwatersheds, this study calibrated
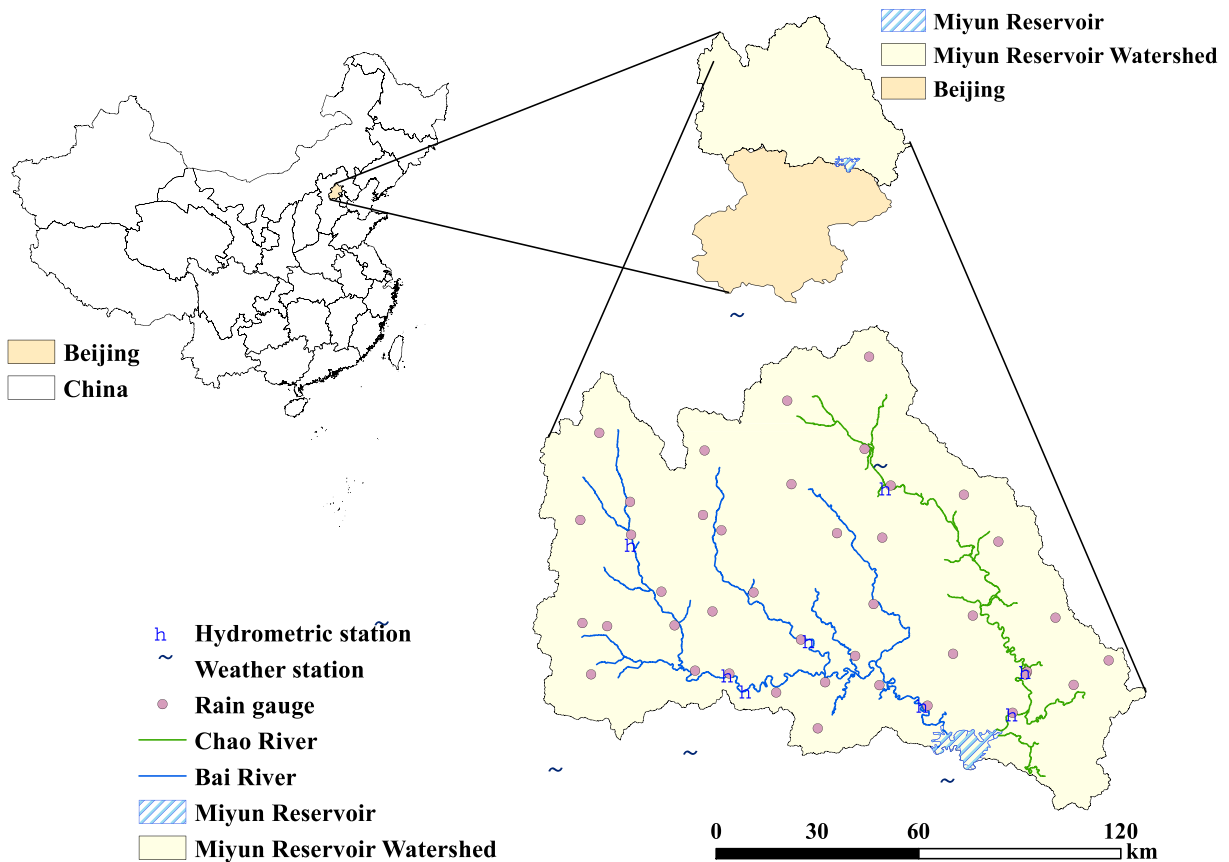
Fig. 1 The location of the Miyun Reservoir Watershed

the model in the Chao River subwatershed and the Bai River subwatershed separately.

The model performance indicators were used to assess the agreement between the observed and simulated data, including Nash-Sutcliffe efficiency coefficient (E_{NS}) (Nash and Sutcliffe 1970) and coefficient of determination (R^2) (Legates and McCabe Jr 1999). The value of E_{NS} varying from $-\infty$ to 1 is defined in Eq. (1). The value of R^2 varying from 0 to 1 is defined in Eq. (2).

$$E_{NS} = 1 - \frac{\sum\limits_{i=1}^{n}(P_i - O_i)^2}{\sum\limits_{i=1}^{n}\left(O_i - \overline{O}\right)^2} \tag{1}$$

$$R^2 = \left[\left(\sum\limits_{i=1}^{n}\left(O_i - \overline{O}\right)\left(P_i - \overline{P}\right)\right) \Big/ \left(\sqrt{\sum\limits_{i=1}^{n}\left(O_i - \overline{O}\right)^2}\sqrt{\sum\limits_{i=1}^{n}\left(P_i - \overline{P}\right)^2}\right)\right]^2 \tag{2}$$

where O_i is the observed data, $\overline{O}$ is the mean value of the observed data, P_i is the simulated value, and $\overline{P}$ is the mean value of the simulated data.

BMP scenarios

The assessment of BMP performance is to calculate the changes in water quantity and quality with or without BMP in multi-spatial and multi-temporal scales by changing the model inputs or parameter values in special modules according to a modeling guide for conservation practices (Waidler et al. 2011; Xie et al. 2015). Several conservation practices were evaluated by the well-calibrated model, including converting farmland to forestland (over 15° slope and over 25° slope, CFF15 and CFF25); nutrient management practices such as 20% and 30% fertilizer reduction; no-till (conservation tillage); residue management practice; strip cropping; contour farming; filter strips with 5 m, 10 m, and 15 m (FS5m, FS10m, and FS15m); detention basins; constructed wetlands; and grassed waterways. For land-management practices, such as converting cropland to forestland, we changed the land use input of SWAT model by reforesting

Table 1 Description of data used in the SWAT model

Data type	Scale	Data description	Source
Digital Elevation Model	1:250,000	Elevation, channel slopes, and lengths	Institute of Geographical and Natural Resources Research, Chinese Academy of Sciences; National Geomatics Center of China
Land use data	1:100,000	Land use types	Institute of Geographical and Natural Resources Research, Chinese Academy of Sciences
Soil properties	1:1,000,000	Soil physical and chemical properties	FAO Harmonized World Soil Database (http://www.fao.org/soils-portal/soil-survey/soil-maps-and-databases/harmonized-world-soil-database-v12/en/)
Weather data	Daily data	Relative humidity, solar radiation precipitation, maximum and minimum air temperatures, wind speed	Local weather stations
Hydrology and water quality	Monthly data	Flow discharge, concentrations of sediment, and nutrients at catchment outlet	Local environmental monitoring station
Social economical data		Population, economic income, livestock rearing, crop types, tillage patterns, fertilizer application	Field investigation; statistics yearbook

the cropping land with slope over 15° and over 25°. The simulation of no-till was conducted by adjusting the mixing efficiency (EFFMIX) and the mixing depth (DEPTIL) in tillage management file (*till.dat*). In addition, the SCS runoff curve number for soil moisture condition II (CNOP) was changed and the Manning's roughness coefficient for overland flow (OV_N) was increased, which help to decrease runoff and peak flow rate (Waidler et al. 2011). Contour farming and strip cropping practices were simulated by decreasing CN2 value and USLE practice factor (USLE_P) in the schedule management operation file (*.ops*). Furthermore, the Manning's *n* and USLE cropping factor (USLE_C) values in the *.ops* file were adjusted for strip cropping operation. For nutrient management practices, the amount of fertilizer applied in cropland was reduced by 20% and 30% in the management file (*.mgt*). For residue management practice, the CN2 and USLE_C in the *.ops* file were adjusted to slow surface runoff.

In the SWAT model, FS was evaluated in the VFS routine, where the field area to VFS area ratio (FILTER_RATIO), the fraction of total runoff from a field entering the most concentrated 10% of a VFS (FILTER_CON), and the fraction of flow through the most concentrated 10% of fully channelized VFS (FILTER_CH) were adjusted (Arnold et al.

2012a). The width of filter strip represented by FILTERW was set to 5 m, 10 m, or 15 m to calculate interception efficiency. For grassed waterways, the depth of channel (GWATD), the average width (GWATW), the linear parameter for calculating sediment re-entrained in channel sediment routing (GWATSPCON), and Manning's *n* value for overland flow (GWATN) were adjusted to reduce the amount of sediment and nutrients entering rivers. Detention basins was represented by respectively setting the erodibility factor (CH_EROD), the Manning's roughness (CH_N2), the surface area of ponds when filled to principal spillway (PND_PSA), the fraction of sub-basin area that drains to ponds (PND_FR), and the hydraulic conductivity through bottom of ponds (PND_K) in the pond management file (*.pnd*). Constructed wetland was simulated by adjusting several wetland parameters in the *.pnd* file such as the fraction of sub-basin area that drains into the wetland (WET_FR), the initial volume of water in wetlands (WET_VOL), the surface area of the wetland at maximum water level (WET_MXSA), the volume of water stored in wetlands at maximum water level (WET_MXVOL), and the hydraulic conductivity through the bottom of the wetland (WET_K). The description of BMP simulation scenarios is shown in Table 2. More details of BMP scenarios are given in the Supplementary Material.

Table 2 The description of BMP simulation scenarios

Individual BMP scenarios	Parameters	Scenario description
Baseline	Existing condition	Simulations using existing crop management schedules
Contour farming	CN2, USLE_P	Simulations using contour farming, but without any other conservation practices
Strip cropping	CN2, n, USLE_P, USLE_C	Simulations using strip cropping, but without any other conservation practices
Residue management	CN2, USLE_C, SO_RES	Simulations using residue management, but without any other conservation practices
No-till	CN2, EFFMIX, DEPTIL, CNOP	Simulations with no conservation practices, except cropping with no-till
CFF15/CFF25	Percentage and distribution of forestland and farmland	Simulations by reforesting cropland over slope of 15° or 25°, but without any other conservation practices
FR20%/FR30%	Fertilizer amount	Simulations with no conservation practices, except fertilizer application was reduced 20% or 30%
FS5m, FS10m, and FS15m	VFS routine (FILTER_RATIO, TILTER_CON, FILTER_CH) or FILTERW	Simulations with no conservation practices, except with filter strips
Constructed wetland	WET_NSA, WET_NVOL, WET_MXSA, WET_MXVOL, WET_VOL, WET_SED, WET_NSED, WET_K, PSETLW1, PSETLW2, NSETLW1 and NSETLW2, et al.	Simulations with no conservation practices, except constructed wetlands were added
Grassed waterway	GWATD, GWATW, GWATSPCON, GWATN	Simulations with no conservation practices, except grassed waterways were added to secondary channels
Detention basin	CH_EROD, CH_N2 PND_FR, PND_PSA and PND_K	Simulations with no conservation practices, except detention basins were added

In this study, efficiency of each BMP was simulated separately, which was represented as the removal rate (negative value of percent change) of TN and TP loads that was calculated as:

$$E = -\frac{Load_{BMP} - Load_{base}}{Load_{base}} \times 100$$

where $Load_{base}$ is the load with no BMPs, and $Load_{BMP}$ is the load with a BMP implementation.

Results and discussions

Model calibration and validation

To enhance the accuracy and validity of the model, a parameter sensitivity analysis is required to select the key parameters that have a dominant effect on the hydrological and water quality processes both in the streams and on the sub-basins. In this study, the SWAT-CUP program was used to analyze the sensitivity of the parameters associated with runoff, N and P, which employed the global sensitivity analysis method that regresses the Latin hypercube generated parameters against the objective function values (Abbaspour 2007; Abbaspour et al. 2007). The results are shown in Tables 3 and 4 for the Chao River subwatershed and Bai River subwatershed, respectively. According to the results in Table 3, the ranking of sensitivity of parameters for the runoff simulation is as follows: GWQMN > SOL_BD > REVAPMN > ESCO > ALPHA_BNK > CN2 > SOL_Z. Different from that of other studies (Baker and Miller 2013; Chen et al. 2015; Jang et al. 2017; Leta et al. 2015), the results in this study showed that CN2 was less sensitive. Similar results were reported by other studies (Bai et al. 2017; Zhu et al. 2011). In the SWAT model, a modified Soil Conservation Service curve number method (SCS-CN) is used to predict runoff volume from a rainstorm, and the CN2 value indicates the soil moisture conditions in pervious areas, which has substantial effects on the generation of

Table 3 The sensitivity rank of parameters in the Chao River Watershed

Variable	Parameter	Description	Lower limit	Upper limit	Conversion	Rank
FLOW	GWQMN	Threshold water level in the shallow aquifer for the base flow	0	5000	v	1
	SOL_BD	Moist bulk density	0.9	2.5	v	2
	REVAPMN	Threshold depth of water in the shallow aquifer for "revap" to occur (mm)	0	500	v	3
	ESCO	Soil evaporation compensation coefficient	0	1	v	4
	ALPHA_BNK	Baseflow alpha factor for bank storage	0	1	r	5
	CN2	SCS moisture condition II curve number for pervious areas	35	98	v	6
	SOL_Z	Depth from soil surface to the bottom of the layer	-1	1	r	7
	CANMX	Maximum canopy storage	0	100	v	8
	SOL_AWC	Available water capacity of the soil layer	0	1	v	9
	SOL_K	Saturated hydraulic conductivity of the first layer	-0.8	0.8	r	10
	CH_K2	Effective hydraulic conductivity in main channel alluvium	-0.01	500	v	11
	EPCO	Plant uptake compensation factor	0	1	v	12
Sediment	USLE_P	USLE equation support practice factor	0	1	v	1
	USLE_K	USLE equation soil erodibility (K) factor	0	0.65	v	2
	SPEXP	Exponent parameter for calculating sediment re-entrained in channel sediment routing	1	1.5	v	3
	USLE_C	Min value of USLE C factor applicable to the land cover/plant	0.001	0.5	v	4
	SPCON	Linear parameter for calculating the maximum amount of sediment that can be re-entrained during channel sediment routing	0.0001	0.01	v	5
TP	SOL_SOLP	Initial labile (soluble) P concentration in surface soil layer	0	100	v	1
	BC4	Rate constant for decay of organic phosphorus to dissolved phosphorus (1/day)	0.01	0.7	v	2
	PSP	Phosphorus sorption coefficient	0.01	0.7	v	3
	K_P	Michaelis-Menton half-saturation constant for phosphorus	0.001	0.05	v	4
	PPERCO	Phosphorus percolation coefficient	10	17.5	v	5
TN	SOL_NO3	Initial NO_3 concentration in the soil layer	0	100	v	1
	BC2	Rate constant for biological oxidation NO_2 to NO_3 (1/day)	0.2	2	v	2
	BC3	Rate constant for hydrolysis of organic nitrogen to ammonia (1/day)	0.02	0.4	v	3
	ERORGN	Organic N enrichment ratio	0	5	v	4
	SOL_ORGN	Initial humic organic nitrogen in the soil layer	0	100	v	3

surface runoff and water balance (SCS 1993). The decreasing precipitation and the low available water capacity of soil layer led to low sensitivity of CN2 in this watershed. In addition, parameters related to groundwater processes (GWQMN and REVAPMN) were sensitive because the water balance system in this watershed is characterized by large contributions of groundwater to streamflow in non-flood season due to the decreasing annual precipitation (Li et al. 2016). SOL_NO3 and SOL_SOLP were identified as the most sensitive parameter for N and P simulations. The initial concentrations of nitrate and soluble P in the soil were in the high degree of sensitivity; these results are consistent with previous studies (Shen et al. 2014; Shrestha et al. 2012). Watershed characteristics and local factors determined the specific parameter sensitivity results that were inapplicable to other watersheds. The sensitive parameters identified in Bai River subwatershed were similar to those in Chao River subwatershed owing to the similar surface characteristics and meteorological conditions within the MRW (see Table 4). The most sensitive parameters were selected for model calibration and validation in the SWAT-CUP program.

The R^2 values and E_{NS} values were used to evaluate the acceptability of the model performance, which are shown in Table 5. According to the results, the R^2 and

Table 4 The sensitivity rank of parameters in the Bai River Watershed

Variable	Parameter	Description	Lower limit	Upper limit	Conversion	Rank
FLOW	SOL_Z	Depth from soil surface to the bottom of the layer	− 1	1	r	1
	CH_K2	Effective hydraulic conductivity in main channel alluvium	− 0.01	500	v	2
	SLSUBBSN	Average slope length	10	150	v	3
	CN2	SCS moisture condition II curve number for pervious areas	35	98	v	4
	SOL_K	Saturated hydraulic conductivity of the first layer	− 0.8	0.8	r	5
	GWQMN	Threshold water level in the shallow aquifer for the base flow	0	5000	v	6
	TRNSRCH	Fraction of transmission losses from main channel that enter deep aquifer	0	1	v	7
	EPCO	Plant uptake compensation factor	0	1	v	8
	CANMX	Maximum canopy storage	0	100	v	9
	SOL_AWC	Available water capacity of the soil layer	0	1	v	10
	GW_DELAY	Groundwater delay (days)	0	500	v	11
	REVAPMN	Threshold depth of water in the shallow aquifer for "revap" to occur (mm)	0	500	v	12
	RCHRG_DP	Deep aquifer percolation fraction	0	1	v	13
Sediment	USLE_P	USLE equation support practice factor	0	1	v	1
	USLE_K	USLE equation soil erodibility (K) factor	0	0.65	v	2
	SPEXP	Exponent parameter for calculating sediment re-entrained in channel sediment routing	1	1.5	v	3
	SPCON	Linear parameter for calculating the maximum amount of sediment that can be re-entrained during channel sediment routing	0.0001	0.01	v	5
	USLE_C	Min value of USLE C factor applicable to the land cover/plant	0.001	0.5	v	4
TP	SOL_SOLP	Initial labile (soluble) P concentration in surface soil layer	0	100	v	1
	ERORGP	Organic P enrichment ratio	0	5	v	2
	BC4	Rate constant for decay of organic phosphorus to dissolved phosphorus (1/day)	0.01	0.7	v	3
	AI2	Fraction of algal biomass that is phosphorus	0.01	0.02	v	4
	SOL_ORGP	Initial humic organic phosphorus in the soil layer	0	100	v	5
TN	SOL_NO3	Initial NO_3 concentration in the soil layer	0	100	v	1
	RS4	Rate coefficient for organic N settling in the reach at 20 °C (1/day)	0.001	0.1	v	2
	AI6	Rate of oxygen uptake per unit NO2-N oxidation	1	1.14	V	3
	CH_N2	Michaelis-Menton half-saturation constant for nitrogen	0.01	0.3	V	4
	NPERCO	Nitrogen percolation coefficient	0	1	v	3

E_{NS} values were consistent with other application in the literature reports (Ahmadzadeh et al. 2016; Chen et al. 2016; Qiu et al. 2018a; Radcliffe and Mukundan 2017; Shrestha et al. 2016), with a range of 0.53–0.88 and 0.44–0.84, respectively, which indicates that the performance of the SWAT model was satisfactory and applicable to the simulation of flow and NPS pollution in these two subwatersheds. The disagreement between the simulated and observed data may result from the unpredictable agricultural activities and management, the limitation in precipitation representation, the impacts of the regular water withdrawals from the upstream reservoirs,

and uncertainties from the model structure and input data (Abbaspour et al. 2015; Leta et al. 2015). This study did not ensure the accuracy of the predicted water storage, and inflow and outflow of these small reservoirs in the simulation process due to the lack of observed data. There are more reservoirs and fewer weather stations in the Bai River subwatershed; this is the important reason that the values of model performance indicators (R^2 and E_{NS}) in the Bai River subwatershed were lower than those in the Chao River subwatershed. Additionally, the transferred amount of flow and pollutant from channel to the base flow and groundwater system could

Table 5 The calibration and validation results at the subwatershed outlets

Variable	Index	Chao River		Bai River	
		Calibration	Validation	Calibration	Validation
Flow (m³/s)	R^2	0.876	0.722	0.635	0.541
	Ens	0.836	0.503	0.591	0.486
TN (kg)	R^2	0.731	0.628	0.592	0.620
	Ens	0.531	0.487	0.525	0.441
TP (kg)	R^2	0.812	0.773	0.634	0.528
	Ens	0.788	0.528	0.528	0.497

not be monitored and validated in the time series. The model accuracy in the flow simulation directly affected the simulation of nutrients and pollutants.

The parameter values differ greatly between these two watersheds. The CN2, SOL_BD, and SOL_K values in the Bai River subwatershed are higher than those in the Chao River subwatershed, which is related to larger surface runoff in the Bai River. However, the GW_DELAY, SOL_AWC, CWQMN, CANMX, REVAPMN, and ESCO values are smaller in the Bai River subwatershed. The proportion of farmland in the Bai River subwatershed is slightly higher than that in the Chao River subwatershed, which resulted in more runoff given its larger CN2. In the Chao River subwatershed, the land use types are dominated by forestland (including economic forest) (50.29%) where the vegetation has important ecological function on water and soil conservation. However, the larger area of barren land with soil erosion contributed to large nutrient loads in this subwatershed. The differences in parameter values account for the discrepancy in the effects of the same conservation practice between these two subwatersheds.

Influencing factors analysis

The relationship between precipitation and temporal distribution of pollutant loads

The temporal distribution of annual and monthly pollutant loads could be used to identify the relationship between precipitation and nutrient losses (see Fig. 2). Precipitation is the driving force for NPS pollution. During rainstorm events, substantial nutrient and sediment losses are caused by surface runoff and leaching, especially in the agricultural areas with extensive use of

fertilizers and frequent cultivation (Abbaspour et al. 2015; Li et al. 2017; Prosdocimi et al. 2016). As shown in Fig. 2 a, b, and c, there is a good linear relationship between annual precipitation and runoff ($R^2 = 0.929$, statistical significance identified by $p < 0.05$) and both TN and TP loads were increasing along with the increase of annual precipitation, which approached a linear relationship ($R^2 = 0.630$ and $R^2 = 0.636$, respectively), e.g., high values of runoff and nutrient loads were observed in typical wet years due to the large precipitation volume (1990 and 1998), whereas the values were low in typical dry years (2002–2005). However, the findings shown in Fig. 2 also imply that precipitation is not the exclusive influencing factor on the nutrient loss from the surface, and other factors, such as fertilizer types, amount and duration of exposure, and even changes in land covers and tillage patterns, have significant impacts on the temporal distribution of nutrient loads (Adimassu et al. 2017; Jakrawatana et al. 2017). This can be explained by the uneven distribution of mean monthly nutrient loads. Figure 2 e and f show that the monthly nutrient loads are not linearly correlated with precipitation, although runoff had a linear correlation with precipitation (Fig. 2d, $R^2 = 0.756$, $p < 0.05$).

As shown in Fig. 3 a, the rainfall was concentrated in the period from May to September, which contributed to the heavy runoff and nutrient loads for the year. The inter-annual distributions of pollution loads indicated a seasonal variation of a low level in the dry period and a sharp increase from the normal-flow period to the flood period; this result was consistent with previous studies (Du et al. 2014; Ylöstalo et al. 2016). As shown in Fig. 3 b, the high nutrient loads in March revealed that after a dry period there was a "first flush effect," which refers to rapid changes in water quality after early-season rains (Gupta and Saul 1996). Within one year, the periods for
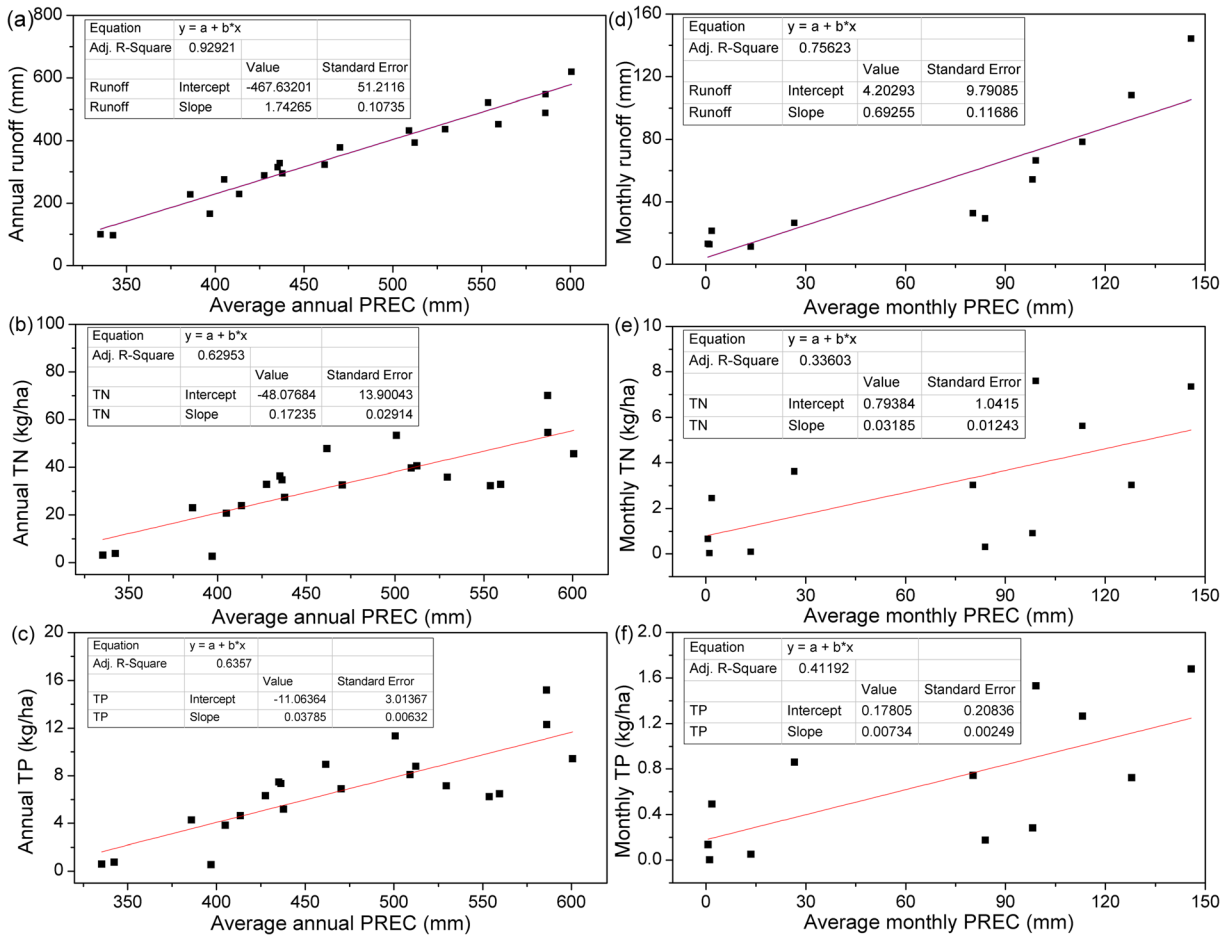
Fig. 2 The relationship between precipitation and variables: annual runoff (**a**), annual TN (**b**), and annual TP (**c**); monthly runoff (**d**), monthly TN (**e**), and monthly TP (**f**)

frequent cultivation, fertilization, and harvesting were distributed in different months (from April to October), which were the critical periods for soil erosion and

nutrient losses along with increasing precipitation. In the MRW, with the application of base fertilizer, corn was planted in May and harvested in September or
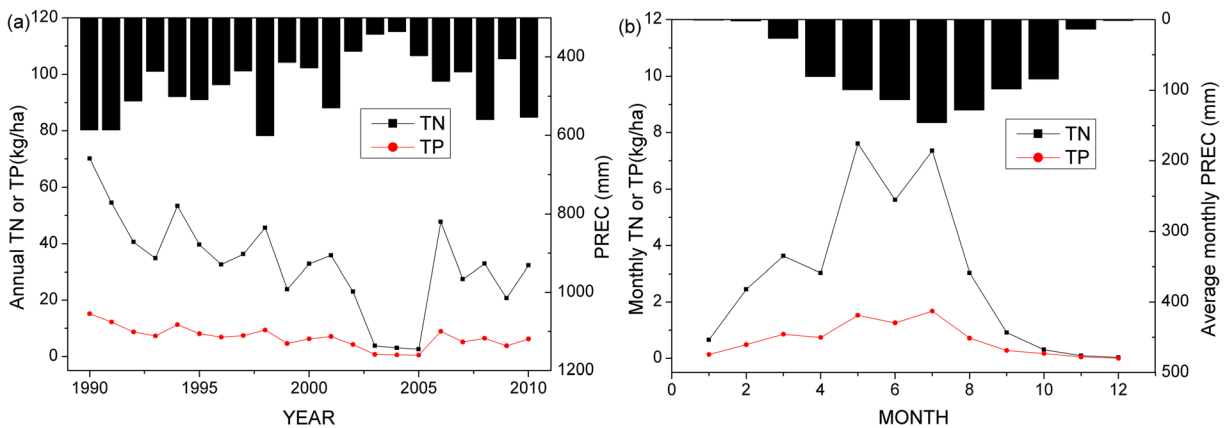
Fig. 3 Temporal distributions of pollutant loads: annual TN and TP loads (**a**), monthly TN and TP loads (**b**)

October; thus, the high nutrient losses in May were caused by the timing of planting, fertilizer application, and soil disturbance.

The spatial distribution of pollutant loads and influencing factors related to land uses

The spatial distributions of the mean annual runoff and NPS pollution loads from 1990 to 2010 are shown in Fig. 4, which demonstrated that NPS pollution had apparent spatial heterogeneity. The spatial distributions of runoff and different pollutants were in agreement with the spatial distributions of land uses. The runoff and nutrient losses were higher in the sub-basins where agricultural land accounted for a large area. These results were consistent with the results of other studies (Cerdà et al. 2016; Ockenden et al. 2017). The land use map is shown in Fig. S1 in the Supplementary Material.

Land use has significant effects on water quality through NPS pollutants within a watershed (Cerdà et al. 2016; Wu et al. 2012). Figure 5 illustrates the nutrient load intensities from different land uses. The nutrient losses were most serious in agricultural land, due to conventional ploughing in sloping terrain, lower vegetation coverage, soil disturbance, the application of pesticides, nitrate and phosphate fertilizers and manures, and soil compaction and sealing on cropping land. Additionally, barren lands were also associated with high load intensities of nutrients, where soil erosion and nutrient loss is prone to occur owing to low vegetation cover and intensive disturbances by composting activities and garbage disposals in this watershed. These results are consistent with previous studies (Bu et al. 2014; Shen et al. 2013). Additionally, forestland and pastureland released relatively high amounts of nutrients, which might result from the use of manure (200 kg/ha set in the SWAT model) in economic forests to enhance the production of dry fruit, such as walnuts and chestnuts, and the high-intensive soil disturbance caused by grazing within pastureland.

The spatial distribution of pollutant loads and influencing factors related to soil types

As stated in previous studies, the soil characteristics and properties are critical factors that affect when and where runoff and diffuse pollution occurs (Fuka et al. 2016). The spatial variation of soil properties directly determines the spatial distributions of nutrient loss, thereby providing significant information for land-management decisions. The nutrient load intensities on different soils is shown in Fig. 6. The nutrient losses from several types of soil were high, including calcaric Cambisols (CMc), eutric Cambisols (CMe), haplic Greyzems (GRh), and luvic Kastanozems (KSl). This is associated with their properties implicated by hydrologic groups C or D that indicate weak ability of water conservation, and fertility preservation due to small soil porosity, slow infiltration rate, strong penetration, and high potential to runoff generation. These soil types are dominated by Cambisols and Regosols, which are intensively used for agricultural production and grazing land in northern China. Cambisols concentrated in temperate regions are the most productive soils distributed in mountainous terrain along with active erosion association with other mature tropical soils (FAO 2016). Farmers apply large amounts of fertilizers to make the soils fertile in order to produce large crop yields. The Regosols are distributed mainly in eroding lands of mountainous regions with steep slope, particularly in the dry tropics, where the soil erosion is combined with wind erosion and water erosion (FAO 2016). In this regard, a large amount of nutrient leaches into water bodies when Regosols are concentrated in the high-intensive irrigated areas.

Efficiencies of BMPs

The simulation results revealed that nutrient loss in the MRW was serious. Average reduction of at least 85.91% of TN load in the Chao River is necessary to comply with the surface-water quality standard (No. GB38382002) that stipulates the limit of TN concentration which is 0.5 mg/L, and reduction of at least 68.53% is necessary in the Bai River, because of the massive use of fertilizers (high N) and manure and a poor wastewater treatment system. Although TP does not exceed the designated water quality standards (0.1 mg/L) at mounts of the Chao River and Bai River, we included it as an important environmental indicator to assess the BMP efficiencies in the MRW. Considering the impacts of land covers and nutrient losses from soil on water quality, a stricter land use program and other practice for source control and water quality restoration should be implemented for integrated watershed management. The monthly TN and TP loads under different BMP scenarios were simulated in SWAT. Generally, the efficiencies of most structural BMPs in the Bai River subwatershed are slightly lower than those in the Chao
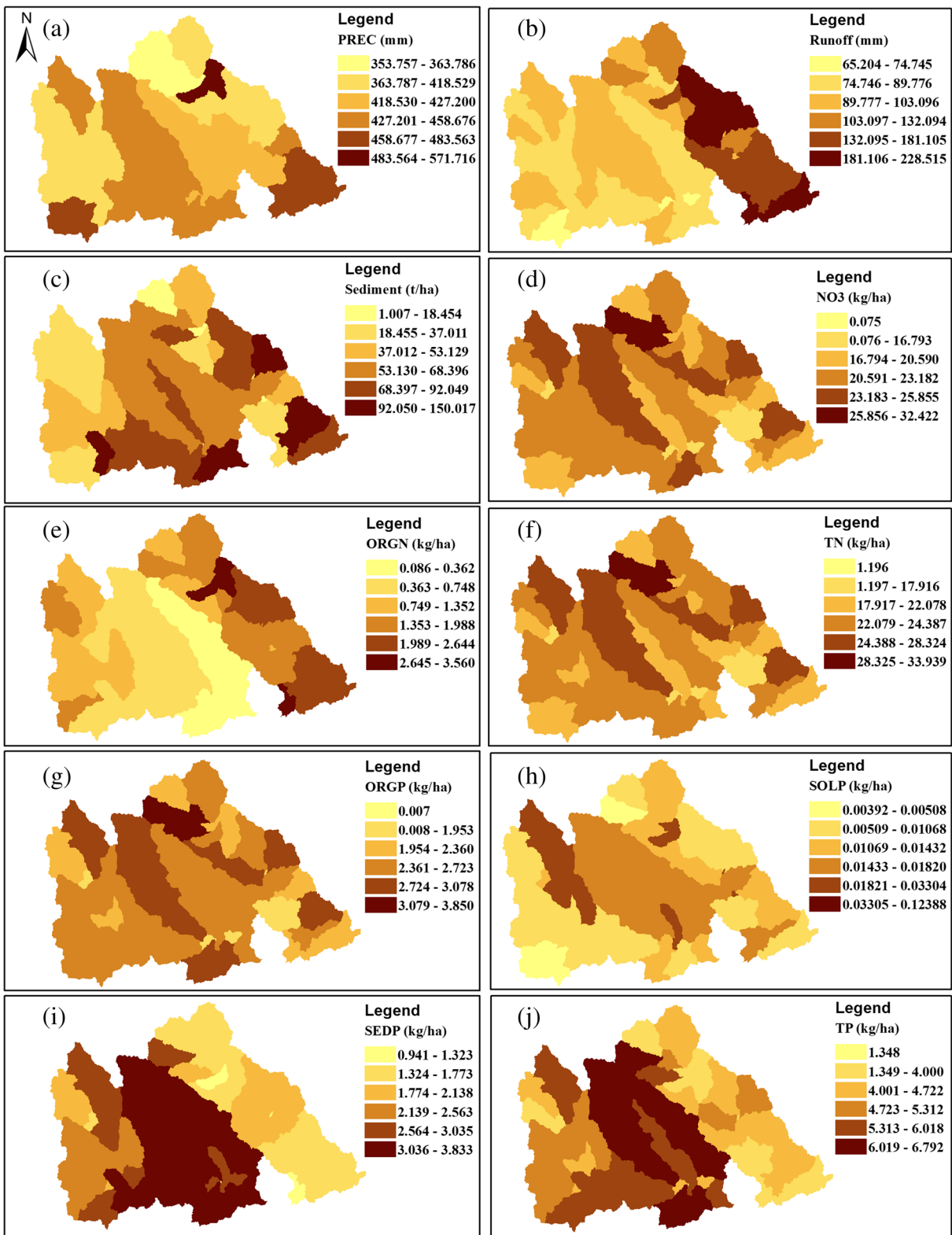
Fig. 4 Spatial distribution of average annual precipitation (PREC) (a), runoff (b), sediment (c), nitrate nitrogen (NO₃) (d), organic nitrogen (ORGN) (e), total nitrogen (TN) (f), organic phosphorus (ORGP) (g), soluble phosphorus (SOLP) (h), and mineral phosphorus attached to sediment (SEDP) (i) and total phosphorus (TP) (j)
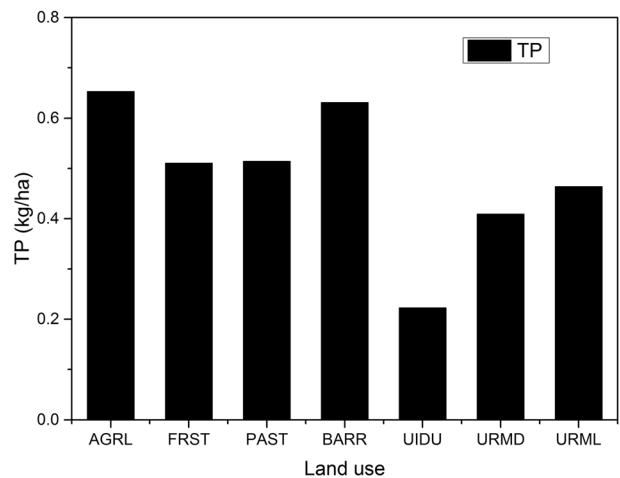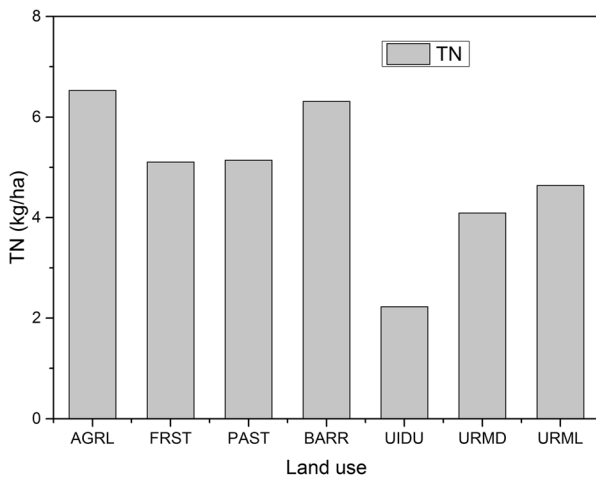
Fig. 5 The relationship between land uses and nutrient loads. AGRL means agricultural land, FRST means mixed forest, PAST means pasture, BARR means vacant land, UIDU means industrial land, URMD means residential land with medium density, and URML means residential with med/low density

River subwatershed. The higher CN2 (higher runoff) and the slightly lower concentration in the Bai River are the main reasons. A rapid runoff on slopes leads to short retention time of runoff flowing over these structures, which is adverse to their effectiveness. This result was consistent with other studies (Fonseca et al. 2018; Jayakody et al. 2014; Liu et al. 2017). However, the land use management practices for controlling nutrient losses in the Bai River subwatershed were more effective than those in the Chao River subwatershed because the proportion of agricultural land that was targeted for re-planning was higher in Bai River subwatershed (Table 6), which contributed to greater changes of land covers and pollution sources. The model also showed that different BMPs had significantly different impacts on the reductions of nutrient loads. Generally, the removal efficiencies of structural BMPs such as filter strips, grassed waterways, and constructed wetlands were better than those of non-structural BMPs.

Land use management practices

Integrated watershed management requires the coordination between land uses and water quantity and quality.
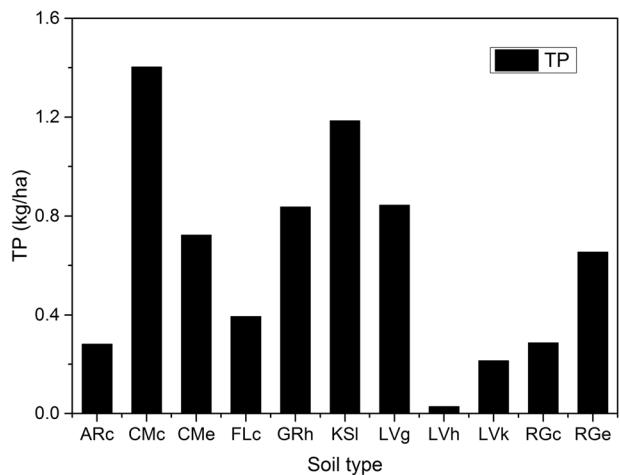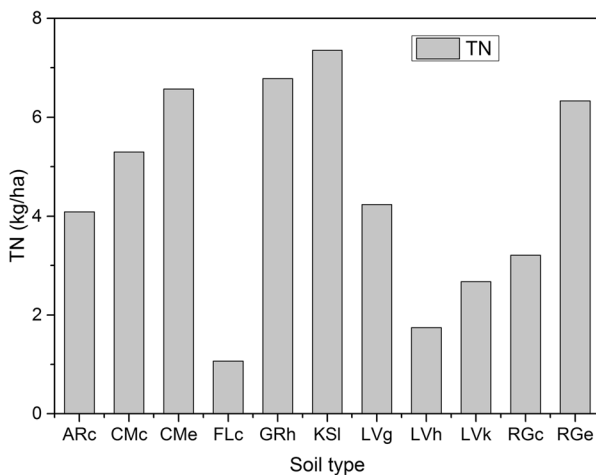
Fig. 6 The relationship between soil types and nutrient loads. ARc represents calcaric arenosols, CMc represents calcaric Cambisols, CMe represents eutric Cambisols, FLc represents calcaric fluvisols, GRh represents haplic Greyzems, KSl represents luvic Kastanozems, LVg represents gleyic luvisols, LVh represents haplic luvisols, LVk represents calcic luvisols, RGe represents eutric Regosols, and RGc represents calcaric Regosols

Table 6 Land use scenarios of converting farmland to forestland (CFF15 and CFF25)

Subwatershed	Land use scenarios	Land use types					
		Cropping land	Forestland	Pastureland	Residential area	Water	Barren land
Chao River	Current land (km^2)	1175.70	3057.65	1526.95	36.75	86.16	9.77
	CFF15 (km^2)	687.67	3545.68	1526.95	36.75	86.16	9.77
	Change ratio (%) of CFF15	− 41.51	15.96	0	0	0	0
	CFF25 (km^2)	996.53	2878.48	1526.95	36.75	86.16	9.77
	Change ratio (%) of CFF25	− 15.24	5.86	0	0	0	0
Bai River	Current land (km^2)	2038.83	4290.85	2551.04	46.38	90.48	13.39
	CFF15 (km^2)	1054.97	5274.71	2551.04	46.38	90.48	13.39
	Change ratio (%) of CFF15	− 48.26	22.93	0	0	0	0
	CFF25 (km^2)	1600.21	4729.47	2551.04	46.38	90.48	13.39
	Change ratio (%) of CFF25	− 21.51	10.22	0	0	0	0

Implementation of eco-friendly tillage patterns, such as residue management and no-till, resulted in very slight improvements in nutrient loss throughout the watershed (Fig. 7). However, in some sub-basins, they resulted in small increases or no significant change in TN and TP losses. This can be explained by the limited surface
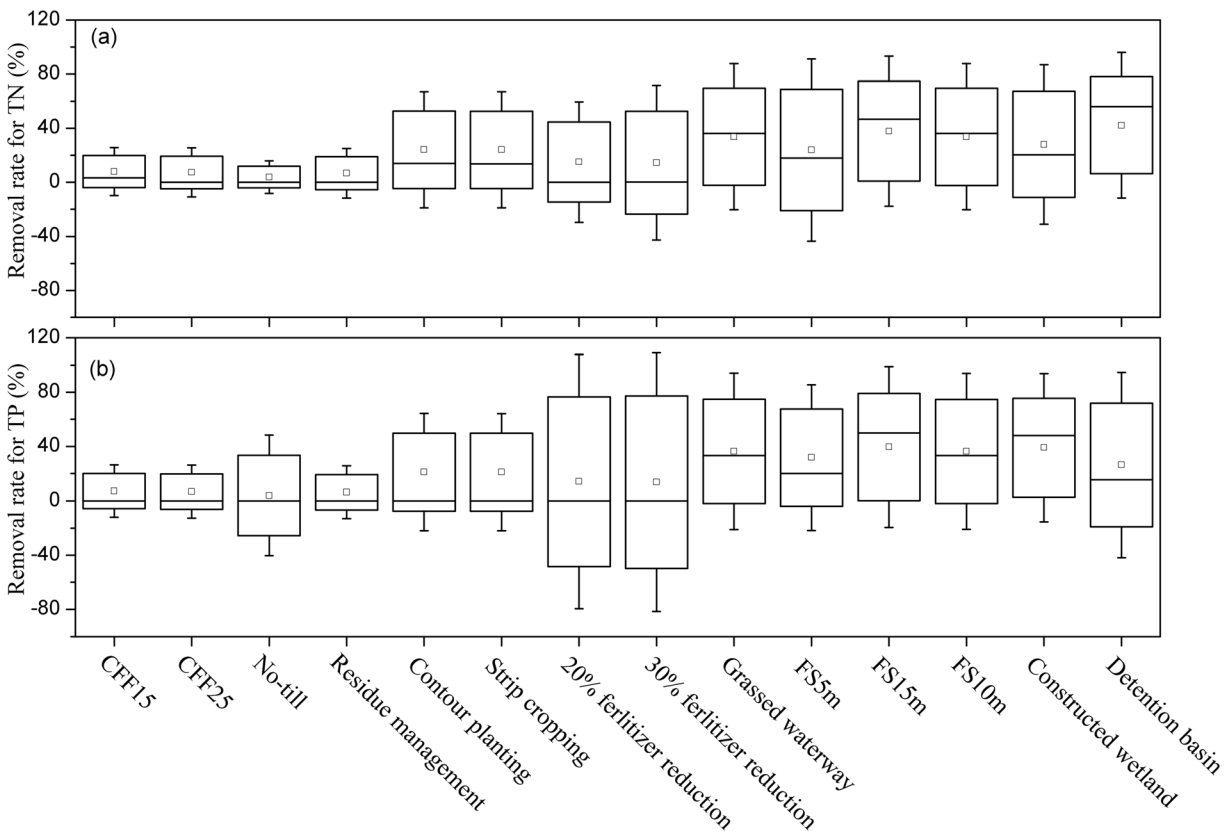
Fig. 7 The monthly efficiency of BMPs for TN load (**a**) and TP load (**b**) among different sub-basins. Point value means the average monthly removal rate of different sub-basins, bar height means the differential between the top quartile and the bottom quartile, and line length means the differential between the highest and the lowest values

runoff and soil erosion and the model limitation that assumes a specific time of tillage for the whole watershed, but this assumption contradicts the actual timing of tillage that varies in different areas within the watershed and depends on local climate conditions and farmer preferences. In addition, the eco-friendly tillage patterns only have the potential to control the small amount of nutrients in the surface and subsurface layers that are available for redistribution by surface runoff. Moreover, increased residues limit soil-disturbing activities, which results in limited incorporation of manures or fertilizers within soils and more nutrient accumulating in topsoil that further increases the amount of nutrient washed out by rainfall and runoff. These results were supported by other studies (Lam et al. 2010; Lam et al. 2011; Taylor et al. 2016; Wallace et al. 2017). The low efficiency can also be attributed to a potential increase in soluble nutrient loads because infiltration and nutrient transport in subsurface flow are increased with more residue cover, and solute nutrients are easily leached through subsurface tiles. It has been found in previous research that solute nutrients are the main components of nutrient losses in the MRW (Qiu et al. 2018b).

The land use change scenarios by CFF15 and CFF25 are shown in Table 6. The croplands with slope over 15° and over 25° slope fields were reforested, respectively. Figure 7 shows that the percent reductions of TN load are similar to those of TP load achieved by CFF practices in this watershed. As previously noted, agricultural lands are the critical sources of water pollution in this watershed. The massive application of fertilizers and manures and frequent activities has caused the release of a large amount of N and P, resulting in the risk of eutrophication in the Miyun Reservoir, particularly from slopping field, where the nutrients are prone to leach into surface runoff accompanied by soil erosion during heavy rain events. The conversion of cropland to forestland on sloped land is part of a national ecological recovery program in China, which has lots of significant ecological impacts, including the minimization of wide-scale soil erosion and vegetation degradation, increases in the soil moisture, reductions in runoff, decreases in the use of fertilizers or manures, and improvements in water quality through the absorption of nutrients or other pollutants by vegetation (Huang et al. 2017; Zhang et al. 2000). The reduction efficiencies of CFF15 for TN and TP loads reached more than 10%, and those of CFF25 were 7–9%. These results are consistent with another study (Liu et al. 2013). Consequently, the small changes

between the baseline scenario and the CFF scenarios can be attributed to the low percentage of slopping fields (22% of the slopping area) that are reforested in this watershed. In addition, reforestation with economic forests was represented in the model by setting a small application of fertilizers and manures and specific logging time in the management operation file, which may increase nutrient losses and soil erosion due to low grass coverage in this afforested area, although there are significant reductions in nutrient losses from cropland.

According to Fig. 7, contour farming and strip cropping on high slope fields (over 15° slope) have similar impacts on nutrient loads. Contour farming involves tillage, planting, and other farm operations along the contour lines to increase water infiltration and reduce runoff, soil erosion, and transport of contaminants (Gao and Yang 2015; Sklenicka et al. 2015; USDA-NRCS 2016). In this study, contour farming reduced mean monthly TN and TP losses by 24.09% and 21.15%, respectively. Compared to other studies (Jeon et al. 2018; Liu et al. 2013), the greater reduction of nutrient loads achieved by contour farming is attributed to the larger area of slopping field that is dominated by dry land, which accounts for 45.79% of the total area of cropland in the MRW. The main crop in sloping fields is corn that has a weak ability to maintain soil and water. Moreover, nutrient losses are easier to induce in dry land than in paddy field, which has been reported in previous studies (Shen et al. 2013). Consequently, the greater reductions of nutrient loads were achieved by contour farming in the sloping fields (dry lands) in the MRW. Consequently, the local conditions, such as slope, crop type, tillage pattern, and soil property, have a substantial effect on the efficiency of contour farming.

Strip cropping, a farming method to conserve soil structure and prevent soil erosion on a steep slope, arranges and cultivates a field into equal width strips with a crop rotation system (USDA-NRCS 2016). In this study, strip cropping reduced mean monthly TN and TP losses by 24.04% and 21.10%, respectively. In contrary to other studies (Fan et al. 2015; Jakrawatana et al. 2017), strip cropping tended to be the most effective at reducing TN than TP in the MRW, due to its capability to reduce surface runoff and erosion and the significantly increased N uptake in plant biomass with the application of urea that is the critical source of N loss. In the MRW, the majority of cultivated land is distributed on hillsides, and the implementation of contour farming and strip cropping can help preserve soil fertility by

minimizing soil erosion as a result of the roots of natural dams holding the soil on the steep slopes. These results indicated that nutrient-use efficiency and soil structure could be improved by strip cropping, which were supported by other studies (Tauchnitz et al. 2018; Wagena and Easton 2018); therefore, strip cropping should be extensively implemented in the MRW.

Nutrient management practices

Based on the on-site questionnaire survey, the current fertilizer amounts applied in cropping land are 325 kg/ha for corn, which would be adjusted in the nutrient management scenarios. The results obtained from the scenarios showed that small (20%) reductions in fertilizer application for arable land resulted in reductions in nutrient loads at the watershed outlet. The simulated values of the reductions in the average monthly loads for TN and TP are 8.22% and 9.74%, respectively. Similar results were obtained in other studies (Lam et al. 2011; Liu et al. 2013). When the fertilizer amount decreased by 30%, the TN and TP loads decreased by 8.73% and 10.20%, respectively. The high content of N in the soil resulted in milder effects of these scenarios on TN than on TP. Nutrient management practices have not covered the fertilizers and manure used in economic forests; this is the primary reason for the relatively low efficiencies of nutrient management practices. Because of the limited data regarding the amount of manure used in this watershed, the control of the amount of chemical fertilizers was applied as a suboptimal nutrient management practice.

Structural best management practices

As shown in Fig. 7, structural BMPs achieved large reductions in TN and TP losses in the sub-basins. Filter strips were added along channels and the edge of fields. The results indicate that filter strip is an effective option to control nutrient losses in these two subwatersheds. Filter strips of 5-m, 10-m, and 15-m width reduced mean monthly TN losses by 23.89%, 37.23%, and 40.42%, respectively, and reduced mean monthly TP losses by 37.01%, 39.34%, and 41.69% in the sub-basins. A reduction in the total area of cropland, a reduction in the total amount of fertilizer and manure applied to cropland within the sub-basin, and a great nutrient transformation/removal by soil microbial processes due to hydrologic pathway alterations are most

likely responsible for the reduction in nutrient losses under buffer strips. These results are consistent with the pollution removal rates of filter strips noted by the Conservation Practices Modeling Guide for SWAT and APEX (Waidler et al. 2011), the values accepted for loading analyses of vegetated filter strips (NHDES 2011), and the findings in other studies (Taylor et al. 2016; Vought et al. 1995). The effectiveness of field strips highly depends on the width of the buffer strips and the extent of the area to which they are applied (Klatt et al. 2017; Stehle et al. 2016). The reductions of nutrient loads increased along with the increase of strip width from 5 to 15 m. As evidenced by our study and the findings of others (Glavan et al. 2012; Klatt et al. 2017), field strips tended to be most effective at reducing TP export than TN. This is due to capability of field strips to reduce surface runoff and surface erosion, which are the primary drivers for sediment associated P export that is the main form of TP losses in the MRW (Qiu et al. 2018b). Furthermore, application of nitrogenous fertilizer (urea) in Cambisols and Regosols soils significantly increases N losses by rainfall-runoff. High TN concentrations in surface runoff can stimulate plant growth in the strips, which results in more P uptake by the plant, and this also partially explains the further reduction in TP by filter strips. These results were supported by other studies (Rousseau et al. 2013; Wagena and Easton 2018).

A constructed wetland is a biological treatment system for sediment retention and nutrient removal that is widely implemented to control streamwater pollution on the urban and watershed scale (USDA-NRCS 2016). As shown in Fig. 7, implementing a constructed wetland within the sub-basin reduced TN and TP losses by 28.03% and 37.83%, respectively. These results have been well documented by previous studies (Ding et al. 2016; Johari et al. 2016; Kuschk et al. 2003), which indicated that the mean removal rates for TN load in a constructed wetland ranged from 10 to 53%, and from 40 to 45% for TP load. The wide ranges of nutrient removal in wetland systems are mainly influenced by the biological process, which depends on plant species, retention times, climatic conditions, soil properties, landscape impact, wastewater types and amount, and system configurations, such as capacity, seasonal storage, and height of embankments (USDA-NRCS 2016; Wu et al. 2015). As previous studies (Ma et al. 2010; Zheng et al. 2016) proposed, the MRW has seen increased precipitation intensity that causes rapid surface

runoff, especially on the slope. The residence time is significantly shortened when water flows across constructed wetlands, which is not conducive to the function of constructed wetlands. The increasing precipitation in winter and decreasing precipitation in summer may have substantial seasonal effects on the efficiency of constructed wetlands, which will be further analyzed in the future.

According to Fig. 7, the removal rate of grassed waterways for TN and TP are 32.67% and 35.02%, respectively, which are close to the efficiencies of filter strips. These results are consistent with the pollution removal rates of grassed waterways noted by the Conservation Practices Modeling Guide for SWAT and APEX (Waidler et al. 2011). Grassed waterways are constructed channels with suitable vegetation for the transport of polluted water and are typically located in agricultural fields (USDA-NRCS 2016). The vegetation can effectively reduce surface erosion, trap sediment, and retain nutrient on the farmlands. As noted in other studies (Qi et al. 2016; Shipitalo et al. 2012; Smith et al. 2015), the removal rates of grassed waterways for N and P loads in surface runoff range from 18.7 to 52.2% and from 19.6 to 52%, respectively. The results of this study fell within the ranges, due to the average slope of the MRW is within the slope interval of these studies. Similar to filter strips, the efficiency of grassed waterways is mainly affected by local conditions and design parameters, such as capacity, stability, width, depth, and slide slopes.

A detention basin is constructed with an engineered outlet to detain sediment-laden runoff, waste solids, and other debris at the site or from other areas (USDA-NRCS 2016). In this study, the removal rates of detention basin for TN and TP loads were 38.36% and 32.60% (see Fig. 7). These results are slightly below the reference values (55% and 68%) in the Conservation Practice Modeling Guide (Waidler et al. 2011). The effect of detention basins on nutrient loads is mainly through reductions in surface runoff and a result of sediment trapping. The loads of sediment and sediment-bound nutrients in surface runoff are relatively lower in the MRW (Fig. 4) than other watersheds (Forsee and Ahmad 2011; USEPA 2009). Thus, a smaller amount of nutrients was detained by detention basins in the MRW. As evidenced by the comparison of our study and the findings of others, the effectiveness of

detention basins is also dependent on local conditions and watershed characteristics.

Conclusions

Agricultural NPS pollution is the major cause of water quality problems in the Miyun Reservoir, the only drinking water source for Beijing. This study used the SWAT model to assess the spatial and temporal distributions of NPS pollution, the factors that affected NPS pollution, and the efficiencies of several conservation practices or BMPs to control nutrient losses. The model determined that the nutrient losses were higher in agricultural land and barren land and were significantly affected by soil properties. The soils with high nutrient losses included Cambisols and Regosols, which are used intensively for agricultural production in northern China. The temporal distribution of pollutant loads was consistent with that of precipitation. Then, the efficiencies of several conservation practices were evaluated using the well-calibrated model, which would help to recommend the appropriate practices for water quality improvement and ecological restoration. The removal efficiencies of structural BMPs such as filter strips, grassed waterways, and constructed wetlands were found to be better than those of nonstructural BMPs, such as residue management, conservation tillage, and nutrient management. The parameter values and the BMP efficiencies differed between the Chao River subwatershed and the Bai River subwatershed owing to slight variances in the land cover, topographic features, and hydrological characteristics.

The findings of this study would be useful to identify the priority control areas and critical control periods of NPS pollution and generate the possible combinations of BMPs to protect drinking water quality in Beijing. Further research is needed to identify the crucial factors that influence the efficiencies of BMPs and extend the potential applications of the BMPs or their combinations that result in the greatest reduction in pollutant loads and requiring the least cost to achieve targeted water quality improvement at watershed scale.

References

Abbaspour, K. (2007). *User manual for SWAT-CUP, SWAT calibration and uncertainty analysis programs*. Eawag, Duebendorf, Switzerland: Swiss Federal Institute of Aquatic Science and Technology.

Abbaspour, K. C., Yang, J., Maximov, I., Siber, R., Bogner, K., Mieleitner, J., Zobrist, J., & Srinivasan, R. (2007). Modelling hydrology and water quality in the pre-alpine/alpine Thur watershed using SWAT. *Journal of Hydrology, 333*(2–4), 413–430.

Abbaspour, K. C., Rouholahnejad, E., Vaghefi, S., Srinivasan, R., Yang, H., & Kløve, B. (2015). A continental-scale hydrology and water quality model for Europe: calibration and uncertainty of a high-resolution large-scale SWAT model. *Journal of Hydrology, 524*, 733–752.

Adimassu, Z., Langan, S., Johnston, R., Mekuria, W., & Amede, T. (2017). Impacts of soil and water conservation practices on crop yield, run-off, soil loss and nutrient loss in Ethiopia: review and synthesis. *Environmental Management, 59*(1), 87–101.

Ahmadzadeh, H., Morid, S., Delavar, M., & Srinivasan, R. (2016). Using the SWAT model to assess the impacts of changing irrigation from surface to pressurized systems on water productivity and water saving in the Zarrineh Rud catchment. *Agricultural Water Management, 175*, 15–28.

Akhavan, S., Abedi-Koupai, J., Mousavi, S.-F., Afyuni, M., Eslamian, S.-S., & Abbaspour, K. C. (2010). Application of SWAT model to investigate nitrate leaching in Hamadan–Bahar Watershed, Iran. *Agriculture, ecosystems & environment, 139*(4), 675–688.

Arnold, J. G., Srinivasan, R., Muttiah, R. S., & Williams, J. R. (1998). Large area hydrologic modeling and assessment Part I: model development. *Journal of the American Water Resources Association, 34*(1), 73–89.

Arnold, J. G., Kiniry, J. R., Srinivasan, R., Williams, J. R., Haney, S. L. & Neitsch, S.L. (2012a). *Soil and water assessment tool input/output documentation, Version 2012*, Texas Water Resources Institute, Temple, TX, USA, TR-439.

Arnold, J. G., Moriasi, D. N., Gassman, P. W., Abbaspour, K. C., White, M. J., Srinivasan, R., Santhi, C., Harmel, R. D., van Griensven, A., Van Liew, M. W., Kannan, N., & Jha, M. K. (2012b). SWAT: model use, calibration, and validation. *Transactions of the ASABE, 55*(4), 1491–1508.

Bai, J., Shen, Z., Yan, T., Qiu, J., & Li, Y. (2017). Predicting fecal coliform using the interval-to-interval approach and SWAT in the Miyun watershed, China. *Environmental Science and Pollution Research, 24*(18), 15462–15470.

Baker, T. J., & Miller, S. N. (2013). Using the Soil and Water Assessment Tool (SWAT) to assess land use impact on water resources in an East African watershed. *Journal of Hydrology, 486*, 100–111.

Bu, H., Meng, W., Zhang, Y., & Wan, J. (2014). Relationships between land use patterns and water quality in the Taizi River basin, China. *Ecological Indicators, 41*, 187–197.

Cerdà, A., González-Pelayo, Ó., Giménez-Morera, A., Jordán, A., Pereira, P., Novara, A., Brevik, E. C., Prosdocimi, M., Mahmoodabadi, M., & Keesstra, S. (2016). Use of barley straw residues to avoid high erosion and runoff rates on persimmon plantations in Eastern Spain under low

frequency–high magnitude simulated rainfall events. *Soil Research, 54*(2), 154–165.

Chen, L., Wei, G., & Shen, Z. (2015). An auto-adaptive optimization approach for targeting nonpoint source pollution control practices. *Scientific reports, 5*, 15393.

Chen, L., Wei, G., & Shen, Z. (2016). Incorporating water quality responses into the framework of best management practices optimization. *Journal of Hydrology, 541*, 1363–1374.

Cronshey, R. G., & Theurer, F. D. (1998). *AnnAGNPS-non point pollutant loading model* (pp. 19–23).

Ding, Y., Wang, W., Liu, X., Song, X., Wang, Y., & Ullman, J. L. (2016). Intensified nitrogen removal of constructed wetland by novel integration of high rate algal pond biotechnology. *Bioresource Technology, 219*, 757–761.

Du, X., Li, X., Zhang, W., & Wang, H. (2014). Variations in source apportionments of nutrient load among seasons and hydrological years in a semi-arid watershed: GWLF model results. *Environmental Science and Pollution Research, 21*(10), 6506–6515.

Fan, F., Xie, D., Wei, C., Ni, J., Yang, J., Tang, Z., & Zhou, C. (2015). Reducing soil erosion and nutrient loss on sloping land under crop-mulberry management system. *Environmental Science and Pollution Research, 22*(18), 14067–14077.

FAO (2016). World Reference Base for Soil Resources: http://www.fao.org/soils-portal/en/.

Faramarzi, M., Abbaspour, K. C., Schulin, R., & Yang, H. (2009). Modelling blue and green water resources availability in Iran. *Hydrological Processes, 23*(3), 486–501.

Ferreira, D. M., Fernandes, C. V. S., Kaviski, E., & Fontane, D. (2019). Water quality modelling under unsteady state analysis: strategies for planning and management. *Journal of Environmental Management, 239*, 150–158.

Fonseca, A., Boaventura, R. A. R., & Vilar, V. J. P. (2018). Integrating water quality responses to best management practices in Portugal. *Environmental Science and Pollution Research, 25*(2), 1587–1596.

Forsee, W. J., & Ahmad, S. (2011). Evaluating urban storm-water infrastructure design in response to projected climate change. *Journal of Hydrologic Engineering, 16*(11), 865–873.

Fuka, D. R., Collick, A. S., Kleinman, P. J. A., Auerbach, D. A., Harmel, R. D., & Easton, Z. M. (2016). Improving the spatial representation of soil properties and hydrology using topographically derived initialization processes in the SWAT model. *Hydrological Processes, 30*(24), 4633–4643.

Gao, S., & Yang, F. (2015). *Rainwater harvesting for agriculture and water supply* (pp. 195–209). Berlin: Springer.

Glavan, M., White, S. M., & Holman, I. P. (2012). Water quality targets and maintenance of valued landscape character–Experience in the Axe catchment, UK. *Journal of Environmental Management, 103*, 142–153.

Gupta, K., & Saul, A. J. (1996). Specific relationships for the first flush load in combined sewer flows. *Water Research, 30*(5), 1244–1252.

Halbe, J., Pahl-Wostl, C., & Adamowski, J. (2018). A methodological framework to support the initiation, design and institutionalization of participatory modeling processes in water resources management. *Journal of Hydrology, 556*, 701–716.

Huang, C., Yang, H., Li, Y., Zhang, M., Lv, H., Zhu, A.x., Yu, Y., Luo, Y., & Huang, T. (2017). Quantificational effect of reforestation to soil erosion in subtropical monsoon regions

with acid red soil by sediment fingerprinting. *Environmental Earth Sciences, 76*(1).

Huber, W.C., Heaney, J.P., Medina, M.A., Peltz, W.A. & Sheikh, H. (1975). *Storm water management model: user's manual, version II.*

Jakrawatana, N., Ngammuangtueng, P., & Gheewala, S. H. (2017). Linking substance flow analysis and soil and water assessment tool for nutrient management. *Journal of Cleaner Production, 142*, 1158–1168.

Jang, S. S., Ahn, S. R., & Kim, S. J. (2017). Evaluation of executable best management practices in Haean highland agricultural catchment of South Korea using SWAT. *Agricultural Water Management, 180*, 224–234.

Jayakody, P., Parajuli, P. B., & Cathcart, T. P. (2014). Impacts of climate variability on water quality with best management practices in sub-tropical climate of USA. *Hydrological Processes, 28*(23), 5776–5790.

Jeon, D. J., Ki, S. J., Cha, Y., Park, Y., & Kim, J. H. (2018). New methodology of evaluation of best management practices performances for an agricultural watershed according to the climate change scenarios: a hybrid use of deterministic and decision support models. *Ecological Engineering, 119*, 73–83.

Jia, L., Zhao, W., Zhai, R., Liu, Y., Kang, M., & Zhang, X. (2019). Regional differences in the soil and water conservation efficiency of conservation tillage in China. *Catena, 175*, 18–26.

Johari, N. E., Abdul-Talib, S., Ab. Wahid, M., & Ab. Ghani, A. (2016). In W. Tahir, P. I. D. S. H. Abu Bakar, M. A. Wahid, S. R. Mohd Nasir, & W. K. Lee (Eds.), *ISFRAM 2015: Proceedings of the International Symposium on Flood Research and Management 2015* (pp. 273–280). Singapore: Springer Singapore.

Klatt, S., Kraus, D., Kraft, P., Breuer, L., Wlotzka, M., Heuveline, V., Haas, E., Kiese, R., & Butterbach-Bahl, K. (2017). Exploring impacts of vegetated buffer strips on nitrogen cycling using a spatially explicit hydro-biogeochemical modeling approach. *Environmental Modelling & Software, 90*, 55–67.

Kuschk, P., Wießner, A., Kappelmeyer, U., Weißbrodt, E., Kästner, M., & Stottmeister, U. (2003). Annual cycle of nitrogen removal by a pilot-scale subsurface horizontal flow in a constructed wetland under moderate climate. *Water Research, 37*(17), 4236–4242.

Lam, Q., Schmalz, B., & Fohrer, N. (2010). Modelling point and diffuse source pollution of nitrate in a rural lowland catchment using the SWAT model. *Agricultural Water Management, 97*(2), 317–325.

Lam, Q. D., Schmalz, B., & Fohrer, N. (2011). The impact of agricultural best management practices on water quality in a North German lowland catchment. *Environmental Monitoring and Assessment, 183*(1-4), 351–379.

Legates, D. R., & McCabe, G. J., Jr. (1999). Evaluating the use of "goodness-of-fit" measures in hydrologic and hydroclimatic model validation. *Water Resources Research, 35*(1), 233–241.

Leta, O. T., Nossent, J., Velez, C., Shrestha, N. K., van Griensven, A., & Bauwens, W. (2015). Assessment of the different sources of uncertainty in a SWAT model of the River Senne (Belgium). *Environmental Modelling & Software, 68*, 129–146.

Li, D., Liang, J., Di, Y., Gong, H., & Guo, X. (2016). The spatial-temporal variations of water quality in controlling points of the main rivers flowing into the Miyun Reservoir from 1991 to 2011. *Environmental Monitoring and Assessment, 188*(1), 42.

Li, Z.-g., Gu, C.-m., Zhang, R.-h., Ibrahim, M., Zhang, G.-s., Wang, L., Zhang, R.-q., Chen, F., & Liu, Y. (2017). The benefic effect induced by biochar on soil erosion and nutrient loss of slopping land under natural rainfall conditions in central China. *Agricultural Water Management, 185*, 145–150.

Liu, H., & Huang, Q. (2013). Adoption and continued use of contour cultivation in the highlands of southwest China. *Ecological Economics, 91*, 28–37.

Liu, R., Zhang, P., Wang, X., Chen, Y., & Shen, Z. (2013). Assessment of effects of best management practices on agricultural non-point source pollution in Xiangxi River watershed. *Agricultural Water Management, 117*, 9–18.

Liu, Y., Engel, B. A., Collingsworth, P. D., & Pijanowski, B. C. (2017). Optimal implementation of green infrastructure practices to minimize influences of land use change and climate change on hydrology and water quality: case study in Spy Run Creek watershed, Indiana. *Science of the Total Environment, 601*, 1400–1411.

Liu, Y., Engel, B. A., Flanagan, D. C., Gitau, M. W., McMillan, S. K., Chaubey, I., & Singh, S. (2018). Modeling framework for representing long-term effectiveness of best management practices in addressing hydrology and water quality problems: Framework development and demonstration using a Bayesian method. *Journal of Hydrology, 560*, 530–545.

Logan, T. J. (1993). Agricultural best management practices for water pollution control: current issues. *Agriculture, Ecosystems & Environment, 46*(1-4), 223–231.

Ma, H., Yang, D., Tan, S. K., Gao, B., & Hu, Q. (2010). Impact of climate variability and human activity on streamflow decrease in the Miyun Reservoir catchment. *Journal of Hydrology, 389*(3), 317–324.

Meissner, R., Gebel, M., Hagenau, J., Halbfass, S., Engelke, P., Giessler, M., Duan, S., Lu, B., & Wang, X. (2016). *Integrated water resources management: concept, research and implementation* (pp. 515–539). Berlin: Springer.

Molina-Navarro, E., Hallack-Alegria, M., Martinez-Perez, S., Ramirez-Hernandez, J., Mungaray-Moctezuma, A., & Sastre-Merlin, A. (2016). Hydrological modeling and climate change impacts in an agricultural semiarid region. Case study: Guadalupe River basin, Mexico. *Agricultural Water Management, 175*, 29–42.

Nash, J. E., & Sutcliffe, J. V. (1970). River flow forecasting through conceptual models part I—a discussion of principles. *Journal of Hydrology, 10*(3), 282–290.

NHDES (2011). New Hampshire Department of Environmental Services, Pollutant Removal Efficiencies for Best Management Practices for Use in Pollutant Loading Analysis. http://des.nh.gov/organization/divisions/water/stormwater/documents/wd-08-20a_apxe.pdf.

Ockenden, M. C., Hollaway, M. J., Beven, K. J., Collins, A., Evans, R., Falloon, P., Forber, K. J., Hiscock, K., Kahana, R., & Macleod, C. (2017). Major agricultural changes required to mitigate phosphorus losses under climate change. *Nature Communications*, 8.

Prosdocimi, M., Jordán, A., Tarolli, P., Keesstra, S., Novara, A., & Cerdà, A. (2016). The immediate effectiveness of barley straw mulch in reducing soil erodibility and surface runoff generation in Mediterranean vineyards. *Science of The Total Environment, 547*, 323–330.

Qi, J., Li, S., Li, Q., Xing, Z., Bourque, C. P. A., & Meng, F.-R. (2016). Assessing an enhanced version of SWAT on water quantity and quality simulation in regions with seasonal snow cover. *Water Resources Management, 30*(14), 5021–5037.

Qiu, J., Shen, Z., Huang, M., & Zhang, X. (2018a). Exploring effective best management practices in the Miyun Reservoir Watershed, China. *Ecological Engineering, 123*, 30–42.

Qiu, J., Shen, Z., Wei, G., Wang, G., Xie, H., & Lv, G. (2018b). A systematic assessment of watershed-scale nonpoint source pollution during rainfall-runoff events in the Miyun Reservoir watershed. *Environmental Science and Pollution Research, 25*(7), 6514–6531.

Qiu, J., Shen, Z., Leng, G., Xie, H., Hou, X., & Wei, G. (2019). Impacts of climate change on watershed systems and potential adaptation through BMPs in a drinking water source area. *Journal of Hydrology, 573*, 123–135.

Radcliffe, D. E., & Mukundan, R. (2017). PRISM vs. CFSR Precipitation Data Effects on calibration and validation of SWAT models. *Journal of the American Water Resources Association, 53*(1), 89–100.

Rousseau, A. N., Savary, S., Hallema, D. W., Gumiere, S. J., & Foulon, E. (2013). Modeling the effects of agricultural BMPs on sediments, nutrients, and water quality of the Beaurivage River watershed (Quebec, Canada). *Canadian Water Resources Journal, 38*(2), 99–120.

SCS. (1993). *National engineering handbook, section 4: hydrology, soil conservation service*. Washington DC, USA: USDA.

Shen, Z., Chen, L., Hong, Q., Qiu, J., Xie, H., & Liu, R. (2013). Assessment of nitrogen and phosphorus loads and causal factors from different land use and soil types in the Three Gorges Reservoir Area. *Science of the Total Environment, 454*, 383–392.

Shen, Z., Qiu, J., Hong, Q., & Chen, L. (2014). Simulation of spatial and temporal distributions of non-point source pollution load in the Three Gorges Reservoir Region. *Science of the Total Environment, 493*, 138–146.

Shipitalo, M. J., Bonta, J. V., & Owens, L. B. (2012). Sorbent-amended compost filter socks in grassed waterways reduce nutrient losses in surface runoff from corn fields. *Journal of Soil and Water Conservation, 67*(5), 433–441.

Shrestha, R. R., Dibike, Y. B., & Prowse, T. D. (2012). modeling climate change impacts on hydrology and nutrient loading in the Upper Assiniboine Catchment. *Journal Of the American Water Resources Association, 48*(1), 74–89.

Shrestha, M. K., Recknagel, F., Frizenschaf, J., & Meyer, W. (2016). Assessing SWAT models based on single and multi-site calibration for the simulation of flow and nutrient loads in the semi-arid Onkaparinga catchment in South Australia. *Agricultural Water Management, 175*, 61–71.

Sklenicka, P., Molnarova, K. J., Salek, M., Simova, P., Vlasak, J., Sekac, P., & Janovska, V. (2015). Owner or tenant: who adopts better soil conservation practices? *Land Use Policy, 47*, 253–261.

Small, G. E., Niederluecke, E. Q., Shrestha, P., Janke, B. D., & Finlay, J. C. (2018). The effects of infiltration-based stormwater best management practices on the hydrology

and phosphorus budget of a eutrophic urban lake. *Lake and Reservoir Management*, 1–13.

Smith, L. E., & Siciliano, G. (2015). A comprehensive review of constraints to improved management of fertilizers in China and mitigation of diffuse water pollution from agriculture. *Agriculture, Ecosystems & Environment, 209*, 15–25.

Smith, D. R., Francesconi, W., Livingston, S. J., & Huang, C.-h. (2015). Phosphorus losses from monitored fields with conservation practices in the Lake Erie Basin, USA. *Ambio, 44*, S319–S331.

Srinivasan, R., Ramanarayanan, T. S., Arnold, J. G., & Bednarz, S. T. (1998). Large area hydrologic modeling and assessment part II: model application. *JAWRA Journal of the American Water Resources Association, 34*(1), 91–101.

Stehle, S., Dabrowski, J. M., Bangert, U., & Schulz, R. (2016). Erosion rills offset the efficacy of vegetated buffer strips to mitigate pesticide exposure in surface waters. *Science of the Total Environment, 545*, 171–183.

Sun, L., Wang, S., Zhang, Y., Li, J., Wang, X., Wang, R., Lyu, W., Chen, N., & Wang, Q. (2018). Conservation agriculture based on crop rotation and tillage in the semi-arid Loess Plateau, China: effects on crop yield and soil water use. *Agriculture, Ecosystems & Environment, 251*, 67–77.

Tauchnitz, N., Bischoff, J., Schrodter, M., Ebert, S., & Meissner, R. (2018). Nitrogen efficiency of strip-till combined with slurry band injection below the maize seeds. *Soil & Tillage Research, 181*, 11–18.

Taylor, S. D., He, Y., & Hiscock, K. M. (2016). Modelling the impacts of agricultural management practices on river water quality in Eastern England. *Journal of Environmental Management, 180*, 147–163.

USDA-NRCS (2016). National Conservation Practices Standards. https://www.nrcs.usda.gov/wps/portal/nrcs/detailfull/national/technical/cp/ncps/?cid=nrcs143_026849.

USEPA (2009). STEPL BMP efficiency rates: extended wet detention.

Volk, M., Bosch, D., Nangia, V., & Narasimhan, B. (2016). SWAT: agricultural water and nonpoint source pollution management at a watershed scale. *Agricultural Water Management, 175*, 1–3.

Vought, L. B.-M., Pinay, G., Fuglsang, A., & Ruffinoni, C. (1995). Structure and function of buffer strips from a water quality perspective in agricultural landscapes. *Landscape and urban planning, 31*(1-3), 323–331.

Wagena, M. B., & Easton, Z. M. (2018). Agricultural conservation practices can help mitigate the impact of climate change. *Science of The Total Environment, 635*, 132–143.

Waidler, D., White, M., Steglich, E., Wang, S., Williams, J., Jones, C., & Srinivasan, R. (2011). *Conservation practice modeling guide for SWAT and APEX*. Texas Water Resources Institute.

Wallace, C. W., Flanagan, D. C., & Engel, B. A. (2017). Quantifying the effects of conservation practice implementation on predicted runoff and chemical losses under climate change. *Agricultural Water Management, 186*, 51–65.

Wu, L., Long, T.-Y., & Cooper, W. J. (2012). Simulation of spatial and temporal distribution on dissolved non-point source nitrogen and phosphorus load in Jialing River Watershed, China. *Environmental Earth Sciences, 65*(6), 1795–1806.

Wu, H., Zhang, J., Ngo, H. H., Guo, W., Hu, Z., Liang, S., Fan, J., & Liu, H. (2015). A review on the sustainability of

constructed wetlands for wastewater treatment: design and operation. *Bioresource Technology, 175*, 594–601.

Xia, X., Wu, Q., Zhu, B., Zhao, P., Zhang, S., & Yang, L. (2015). Analyzing the contribution of climate change to long-term variations in sediment nitrogen sources for reservoirs/lakes. *Science of the Total Environment, 523*, 64–73.

Xie, H., Chen, L., & Shen, Z. (2015). Assessment of agricultural best management practices using models: current issues and future perspectives. *Water, 7*(3), 1088–1108.

Yen, H., White, M. J., Arnold, J. G., Keitzer, S. C., Johnson, M. V. V., Atwood, J. D., Daggupati, P., Herbert, M. E., Sowa, S. P., Ludsin, S. A., Robertson, D. M., Srinivasan, R., & Rewa, C. A. (2016). Western Lake Erie Basin: Soft-data-constrained, NHDPIus resolution watershed modeling and exploration of applicable conservation scenarios. *Science of the Total Environment, 569*, 1265–1281.

Ylöstalo, P., Seppälä, J., Kaitala, S., Maunula, P., & Simis, S. (2016). Loadings of dissolved organic matter and nutrients from the Neva River into the Gulf of Finland – biogeochemical composition and spatial distribution within the salinity gradient. *Marine Chemistry, 186*, 58–71.

Zhang, P., Shao, G., Zhao, G., Le Master, D. C., Parker, G. R., Dunning, J. B., & Li, Q. (2000). China's forest policy for the 21st century. *Science, 288*(5474), 2135–2136.

Zheng, J., Sun, G., Li, W., Yu, X., Zhang, C., Gong, Y., & Tu, L. (2016). Impacts of land use change and climate variations on annual inflow into the Miyun Reservoir, Beijing, China. *Hydrology and Earth System Sciences, 20*(4), 1561–1572.

Zhu, L., Qin, F., Yao, Y., Zhang, L., & Yu, X. (2011). Research of sensitivity analysis module of SWAT model in middle-scale watershed——a case study of Hongmenchuan Watershed in Miyun County. *Research of Soil and Water Conservation, 18*(1), 161–165,275.

Zhu, Q., Gould, J., Li, Y., & Ma, C. (2015). *Rainwater harvesting for agriculture and water supply*. Berlin: Springer.